Impact of aeration shear stress on permeate flux and fouling layer properties in a low pressure membrane bioreactor for the treatment of grey water

An Ding [a,b,1], Heng Liang [b,*], Guibai Li [b], Nicolas Derlon [a,c], Ilona Szivak [a], Eberhard Morgenroth [a,c], Wouter Pronk [a,*]

[a] Eawag, Swiss Federal Institute of Aquatic Science and Technology, Überlandstrasse 133, CH-8600 Dübendorf, Switzerland
[b] State Key Laboratory of Urban Water Resource and Environment (SKLUWRE), Harbin Institute of Technology, 73 Huanghe Road, Nangang District, Harbin 150090, PR China
[c] Institute of Environmental Engineering, ETH Zürich, CH-8093 Zürich, Switzerland

ARTICLE INFO

ABSTRACT

Two different aeration regimes were studied in a low pressure gravity driven membrane bioreactor without any flushing or (back-) washing. In one reactor, the aeration was positioned below the membrane module, thus exposing the membranes to aeration shear stress. A second reactor was operated at low shear stress by placing the aerator in a different compartment. Flux stabilization at 2.0 L/(m² h) occurred in the reactor with low shear stress while no flux stabilization was observed in the reactor with aeration shear stress, resulting in a flux of 0.5 L/(m² h) after 120 days. The thickness of the bio-fouling layer in the reactor with aeration shear was smaller (129 vs. 344 μm), which implies that shear stress resulted in a thinner, denser and less permeable bio-fouling layer. The results can be explained by differences in (1) the morphology of the bio-fouling layer and (2) the EPS contents (proteins and polysaccharides) in the bio-fouling layer. The low-shear system provides a suitable solution for decentralized grey water treatment, or other conditions where maintenance and energy consumption should be minimized. Furthermore, the results can contribute to decrease the energy consumption in MBR systems.

© 2016 Elsevier B.V. All rights reserved.

1. Introduction

Membrane bioreactors (MBR) are increasingly being applied for wastewater treatment, especially when a high effluent quality is required, e.g. in the case of water reuse or water recycling [1]. In addition to the effluent quality, MBRs offer advantages in terms of small footprint, low sludge production and modular design. However, MBR processes also have several disadvantages, such as the need for membrane cleaning and the higher capital costs as well as higher operating costs [2]. Peter-Varbanets et al. [3,4] developed low pressure gravity-driven membrane filtration (GDM). The main feature of this system is that it allows formation of a biofilm on the membrane, enabling operation at stable fluxes

during extended periods of time (several months) without any cleaning or flushing at pressures below 0.1 bar. GDM is considered to be a suitable process for decentralized production of drinking water in developing countries and emerging markets [5]. The flux stabilizes at 3–15 L/(m² h) depending on the water quality after several months of operation due to the formation of a highly permeable bio-fouling layer [3,6,7]. This stable flux in GDM systems is fundamentally different from the concept of critical flux, which was first put forward in a microfiltration system by Field et al. [8], and which describes stable flux values during limited time periods only. Additionally, another fundamental difference between the critical and stable flux concept is that the former is typically applied at constant flux operation while the latter is evident at constant pressure operation.

Besides potable water treatment, also grey water treatment will further gain importance in future due to the increasing water shortage in many areas of the world. In this paper we focus on the treatment of grey water using GDM technology. In order to prevent anaerobic conditions, aeration was applied in combination with submerged flat-sheet membranes, resulting in a gravity-
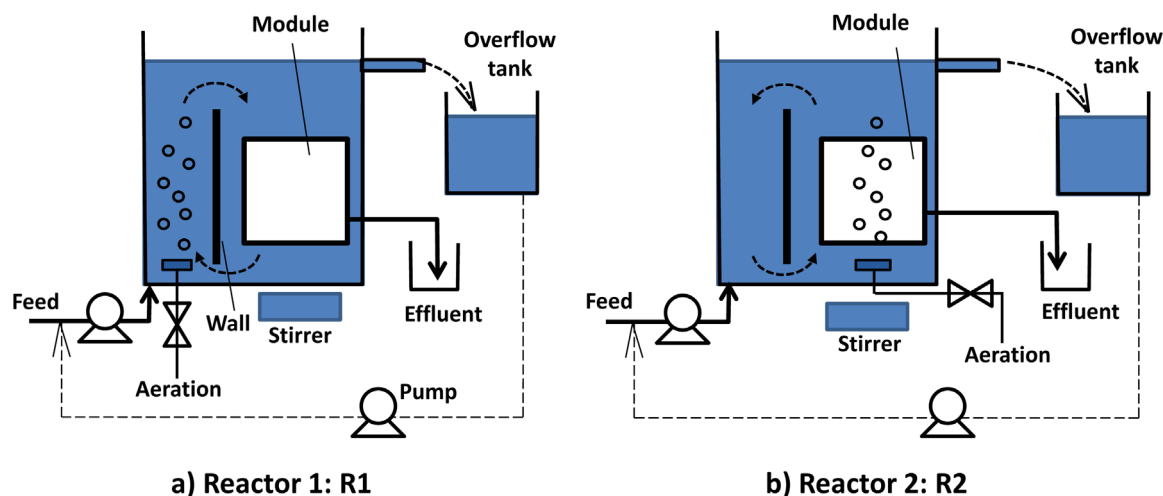
Fig. 1. Schematic diagram of the two membrane systems investigated: (a) R1 low shear at the membrane and (b) R2 with high shear force at the membrane surface. Dashed arrows indicate the liquid flow direction.

driven MBR ("GDMBR").

For MBRs it has been reported that one of the effective measures to retard the membrane fouling is increasing the aeration intensity [2,9,10]. The aeration not only provides oxygen to the biomass, but also maintains the solids in suspension in the activated sludge process [11]. The aeration intensity strongly impacts the mixed liquor organic matter fractions and correspondingly influences the membrane fouling rate [10]. Nywening and Zhou [12] found that the fouling rate decreased exponentially with increasing scouring aeration intensity, and the effects of scouring aeration intensity and permeate flux on the fouling rates were found to be independent of one another. Trussell et al. [13] also reported that increasing the coarse bubble aeration intensity increased the permeability at a given mixed liquor suspended sludge (MLSS) concentration. Furthermore, an optimal air flow rate was reported, and aeration intensity smaller or larger than this optimal value had a negative impact on the membrane permeability [11]. Low aeration intensity could not remove the membrane foulants from the membrane surface effectively. However, a high aeration intensity led to a severe breakup of sludge flocs, and promoted the release of colloids and solutes from the microbial flocs to the bulk solution [11]. Even though shear limits biofouling, the formation of a biofouling layer is never completely avoided in practice. Ultimately, the permeate flux thus steadily decreases.

It is evident that increasing the aeration intensity leads to an increase of the concentration of dissolved oxygen (DO). The concentration of DO influences the properties of the suspended sludge, such as the floc structure, particle size distribution and the content of extracellular polymer substances (EPS), and these factors also have an impact on the membrane permeate flux [14–16]. The fouling rate in a low-DO MBR was compared to a high-DO MBR, while keeping the shear conditions constant in both reactors, showing a 7.5 times faster fouling at low-DO than at high-DO conditions [17]. In the latter study, only the influence of DO concentration was studied, and the effect of shear stress while keeping DO constant has not been reported so far. In GDM systems, the biofouling layer is tolerated, while the hydraulic resistance of the fouling layer is low due to the low pressures applied [3]. Actually, the presence of the biofouling layer is suggested to be a requirement for long-term stabilization of flux in the treatment of river water [3]. In the present investigation, we will evaluate this hypothesis for the treatment of a more concentrated water (grey water). In contrast to GDM of river water, aeration is required in grey water treatment, in order to avoid anaerobic conditions. In GDM, the presence of biofilm is tolerated not only by refraining

from flushing, but also by avoiding shear (dead-end operation). As outlined above, MBRs are usually operated at high shear conditions, for example by placing the aeration directly under the submerged membranes. In order to evaluate our hypothesis of a "protective biofilm", we used a different concept, whereby shear is minimized by placing the aerator in a different compartment, while providing sufficient mixing between membrane compartment and aeration compartment. As a comparison, a system was operated featuring high shear at the membrane surface, using aeration placed directly under the submerged membranes, while maintaining equal DO concentrations in both systems. In order to further investigate the fouling characteristics of these systems, the properties of the biofouling layers were investigated, including the morphology, density and EPS composition.

2. Experimental

2.1. Setup and feed water composition

Two gravity-driven membrane bioreactors were operated in parallel treating synthetic grey water during four months of operation. The reactors were made of polymethyl methacrylate with a working volume of 9 L (Fig. 1). Flat sheet membrane plates were constructed by gluing membranes on both sides to a PVC frame using an epoxy resin. Three membrane plates were applied in each reactor. The effective membrane surface was 10×10 cm, so each plate contained 0.02 m^2 of membrane and the total membrane surface per reactor was 0.06 m^2, and the distance between the modules was 3.0 cm. Membranes were UP150 from Microdyn Nadir (Wiesbaden, Germany), made of polyethersulfone with a nominal cut-off of 150 kDa, which corresponds to a mean pore size of approximately 15 nm. Virgin membranes were cleaned for 24 h in deionized water to remove chemical reagents. Both systems were located in a temperature-controlled room keeping the temperature in the membrane tanks constant at 20 °C.

An aquarium tube diffuser was placed at the bottom of each reactor to provide dissolved oxygen. In addition, a magnetic stirrer was used in each reactor to avoid sludge settling (see Fig. 1). To investigate the effect of aeration shear on the membrane surface, a wall was installed in R1 to separate the aeration diffuser from the membrane modules, whereas the diffuser was placed below the membrane module to provide coarse bubbles in R2 as a control system (Fig. 1). According to the air-lift principle, the aerator generates a gentle liquid circulation between aeration

compartment and membrane compartment, as shown in Fig. 1. It can be assumed that the flow conditions in an aerated bioreactor are turbulent [18], while in R1 a gentle recirculation flow occurs due to the airlift effect (Fig. 1), which results in laminar flow conditions. Thus, R1 is designated as "low-shear", and R2 as "high-shear".

The aeration rate in both reactors was maintained at a constant rate of 60 L/h. Ueda et al. [9] found that air injection reduced fouling in an SMBR up to a critical flow rate corresponding to a Specific Aeration Demand per Membrane area (SADm) of 250 L/h m^2. Beyond this value, increasing airflow did not have a positive effect on TMP, which was linked with the cake removal efficiency. In our study, the SADm was corresponding to 1000 L/h m^2, which is higher than the critical value. The reactor footprint was 450 cm^2, so that the superficial gas velocity in the tank and along the modules can be calculated as 3.7×10^{-4} m/s and 1.7×10^{-3} m/s, respectively. The SRT was infinite in both systems, while the suspended sludge was not discharged during the whole operation.

A synthetic grey water solution was continuously pumped into the reactor and the gravitational pressure head was kept constant at 50 mbar (5 kPa) in each reactor by keeping the liquid level constant using an overflow. The overflow was recycled to the feed pump in such a way to ensure that the feed water flow equalled the permeate flow (see Fig. 1). The composition of the synthetic grey water solution was based on literature [19,20] in order to represent mixed kitchen and shower grey water, and consisted of the following compounds: glucose (250 mg/l), humic acid (2 mg/L), cellulose (10 mg/L), oleic acid (10 mg/L), linoleic acid (10 mg/L), sodium laurylsulfate (5 mg/L), sodium monofluorophosphate (5 mg/L), $CaCl_2 \cdot 2H_2O$, (183 mg/L), NH_4Cl (120 mg/L), KH_2PO_4 (22 mg/L), $NaHCO_3$ (200 mg/L) and a mixture of trace elements. The feed solution contained in total 300 mg COD/L, 100 mg Total Organic Carbon (TOC)/L, 30 mg NH_4^+-N/L and 5 mg TP/L, and a pH value of 7.5–8.0.

2.2. Characterization of the cake layer

2.2.1. Optical Coherence tomography

Optical Coherence Tomography (OCT) with a central light source wavelength of 930 nm was used to investigate the physical structure of the bio-fouling layer using a model 930 nm Spectral Domain OCT (Thorlabs GmbH, Dachau, Germany). For image acquisition, membrane modules were taken out of the reactor and carefully placed on the OCT stage for measurement to avoid structural changes of the layer. OCT images were recorded with the samples immersed in a thin layer of the permeate. 15–20 images of cake layer optical cross sections were acquired at different randomly chosen positions for each membrane module. Matlab® (Math Works, Natick, US) based image analysis was used to analyse OCT images including the thickness and roughness of the fouling layer, as described previously [7].

2.2.2. Confocal laser scanning microscopy (CLSM)

CLSM (Leica SP5, Wetzlar, Germany) was used to investigate the development of the fouling layer structure, especially the organism and EPS distributions in the bio-fouling layer. The membrane modules were taken out for CLSM analyses at the end of GDMBR operation. The fouled membranes were first fixed with formaldehyde solution (2.5%), washed twice with nanopure water and cut in several 1 cm^2 pieces. Then, samples were stained with different dyes, incubated in the dark for half an hour at 20 °C and washed again with pure water. Each piece was scanned three times at different randomly chosen positions. 4'-6-diamidino-2-phenylindole (DAPI) was used to stain the fouling layer to represent the total bacterial cells. Concanavalin A (100 fold diluted stock solution, Invitrogen, Basel, Switzerland) was used to stain

the α-d-mannose and α-d-glucose groups of biopolymers to represent the polysaccharides. Sypro Orange was used to stain proteins. Image analysis was carried out using *Imaris* (Bitplane, Zürich, Switzerland) and *ImageJ* (National Institutes of Health).

2.2.3. Chemical analyses

The TOC of influent and effluent were measured by an automatic total organic carbon analyser (TOC-V, Shimadzu, Japan). DOC of mixed liquor sludge was measured to represent the soluble microbial products (SMP) in the bulk solution. Samples were determined by filtering the sludge through a 0.45 μm filter (Whatmann, Maidstone, UK) and the DOC of the permeate was measured using a TOC analyser (TOC-V, Shimadzu, Japan).

Extraction of extracellular polymeric substances (EPS) from suspended sludge and the sludge from the cake layer was carried out by heating at 80 °C for 30 min, followed by centrifuging at 10,000g for 20 min, and then collecting the supernatants as described by Adav and Lee [21]. The TOC concentration of the supernatant was measured to represent total EPS. The concentration of proteins was measured by the bicinchoninic acid (BCA) method according to Smith et al. [22]. The concentration of polysaccharides was determined by the anthrone-sulphuric method [23]. The analyses were all conducted in duplicate, and their average values were reported.

2.2.4. Dissolved oxygen

The dissolved oxygen (DO) concentration was measured near the membrane surface using a dissolved oxygen meter (Oxi 340i-WTW, Germany). Before each measurement, any biofilm formed on the reactor walls was removed mechanically and resuspended.

2.3. Permeate flux

The permeate flux was calculated as the weight of effluent collected from each system, divided by the specific weight, by the filtration period and by the area of membrane. The mass of permeate was weighed daily using a scale (Ohaus Adventure Pro®, Pine Brook (NJ), USA).

2.4. Evaluation of fouling behaviour

To evaluate the fouling behaviour, Darcy's law was applied to estimate the total fouling resistance as shown in Eq. (1)

$$J = \frac{\Delta P}{\mu R_t} \tag{1}$$

$$R_t = R_m + R_c + R_p \tag{2}$$

$$R_t = R_m + R_r + R_{ir} \tag{3}$$

where J is permeate flux (m^3/(m^2 s)), ΔP is trans-membrane pressure (Pa), μ is the dynamic viscosity (Pa s), and R is the filtration resistance (m^{-1}). As shown in Eq. (2), the total resistance (R_t) can be expressed as the sum of membrane resistance (R_m), pore blocking resistance (R_p) and bio-fouling, or cake resistance (R_c) [24,25]. Alternatively, the total resistance can be expressed as the sum of membrane resistance (R_m), resistance of hydraulically reversible (R_r) and hydraulically irreversible fouling (R_{ir}), as shown in Eq. (3). R_t was measured at the end of the experiment, using the permeate flux of the last day; R_m was determined by measuring the flux of the virgin membrane with nanopure water; R_{ir} and R_r were calculated by testing the flux before and after flushing the membrane surface using nanopure water. R_c and R_p were

calculated by measuring the flux before and after mechanical cleaning of the membrane surface using a sponge. Chemical cleaning was carried out after mechanical cleaning, and the morphology of the residual fouling layer was observed afterwards. Chemical cleaning was performed by immersing the membrane modules in a NaClO solution with the concentration of 0.1% for 24 h.

3. Results

3.1. Organic carbon removal

Reactors R1 and R2 were operated without backwash and hydraulic cleaning at a gravitational trans-membrane pressure of 50 mbar (5 kPa). The aeration rate in both reactors was maintained at a constant value of 60 L/h. The DO concentration near the membrane surface in both reactors decreased from 8.2 mg/L at the start of the experiment to 6.0–6.5 mg/L after 19 days until the end of the experiment. As shown in Fig. 1, the airlift principle provided mixing of both reactors (although small dead zones existed), and thus, homogeneous DO concentrations were obtained, while generating low shear in Reactor 1. Fig. 2(a) and (b) shows the effluent TOC and mixed liquor DOC concentrations of the two

(a)

(b)
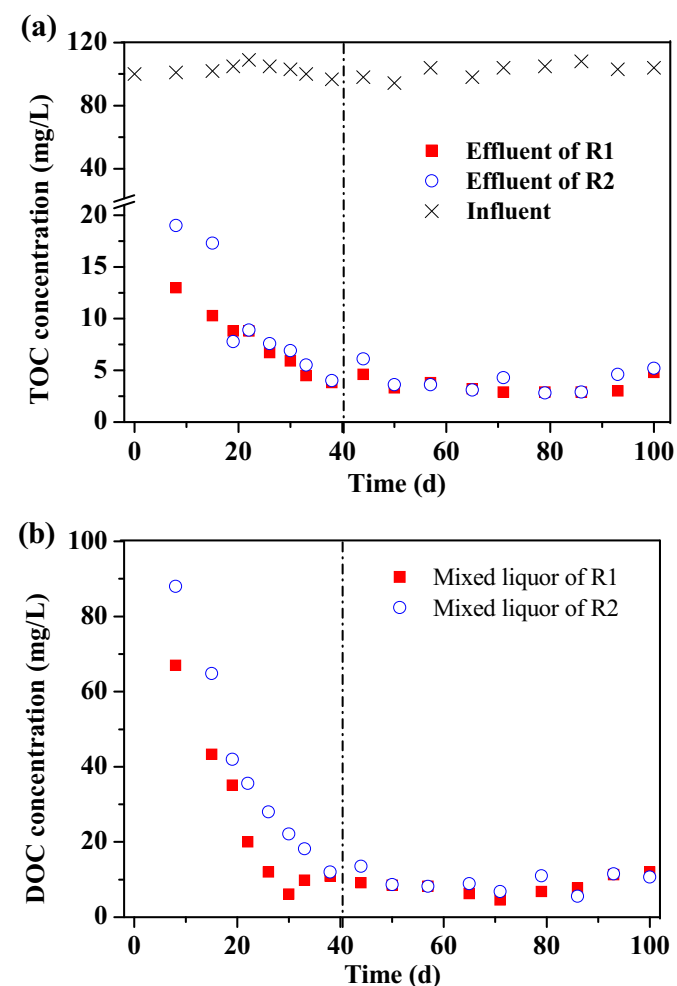
Fig. 2. (a) TOC concentrations in the effluent with time, (b) SMP concentrations (DOC concentrations of mixed liquor) as a function of time. R1 denotes the reactor with low shear stress, R2 the reactor with aeration shear stress. The dashed line indicates the transition between the first stage (0–40 days) and the second stage (40–100 days).
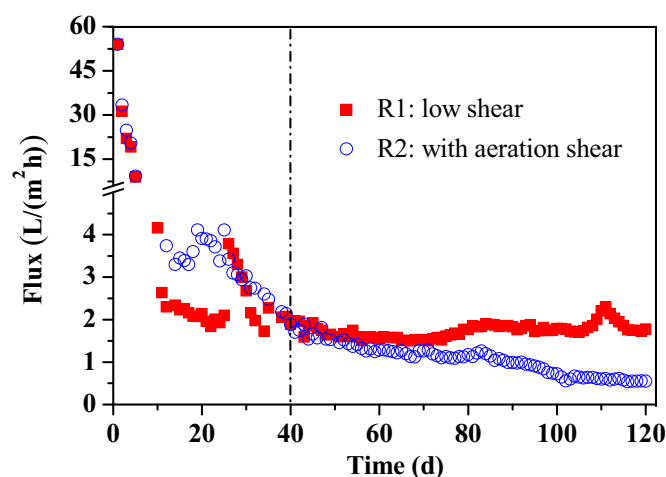
Fig. 3. Flux versus time of R1 (low shear) and R2 (with aeration shear). The dashed line indicates the transition between the first stage (0–40 days) and the second stage (40–100 days). The temperature in both systems was kept stable at 20 °C.

reactors versus time, respectively. Fig. 2(a) can be roughly divided into two stages. During the first stage (the first 40 days operation), the TOC concentrations of the effluent in R1 and R2 decreased rapidly from 20 mg/L to around 5 mg/L. After that (in the second stage), the concentrations were stable around 5 mg/L in both reactors. As for the mixed liquor sludge, Fig. S1 in the Supplementary Material presents the sludge concentration in the two reactors as a function of time. There was no substantial difference between the two systems during the first 80 days of operation, and the sludge concentration increased slightly in both reactors from 0 to around 400 mg/L. During days 80–120 the sludge concentration in R1 (low shear) increased slightly faster than R2 (aeration shear), with final concentrations of 902 mg/L in R1 and 456 mg/L in R2. It can be seen in Fig. 2(b) that the DOC concentration in R1 and R2 dropped sharply from 90 mg/L to 10 mg/L and 65 mg/L to 10 mg/L respectively, during days 0–40. During this period, the DOC concentrations in R2 were always higher than in R1. The reason for this difference might be the lower hydraulic retention time (HRT) in R2, caused by the higher flux in the initial stage (see Fig. 3), leading to an increased organic load. In the second stage, the DOC concentrations of both reactors were stable between 10 and 15 mg/L, and the concentration difference was negligible, although the flux and thus the organic load of both reactors was different from day 60 onwards. This implies that in this period, where the biological activity is fully developed, the residence time is not limiting the degradation of TOC and DOC significantly.

3.2. Effect of aeration shear stress on the permeate flux decline

The permeate flux is plotted against time in Fig. 3. This figure can be roughly divided into two stages. In the first stage (day 0–40), the flux dropped from 50 L/(m² h) to about 2.0 L/(m² h). The permeate flux in R2 (with aeration shear) was always higher than R1 (low shear) in this stage. Flux variations during the period of day 10–25 were due to gas accumulation within the membrane modules in both reactors. This problem was resolved on day 25 by introducing an additional gas outlet on the top of the membrane plates to release the gas. In the second stage (day 40–120), the permeate flux of R1 stabilized at around 2.0 L/(m² h) with slight variations but without a structural change of flux. In contrary, the flux in R2 continued to decrease, and the values were lower than in R1. The flux value in R2 dropped to 0.5 L/(m² h) at the end of the experiment (day 120). From these results, it can be concluded that the permeate flux of synthetic grey water treatment is stabilizing

(a)

(b)
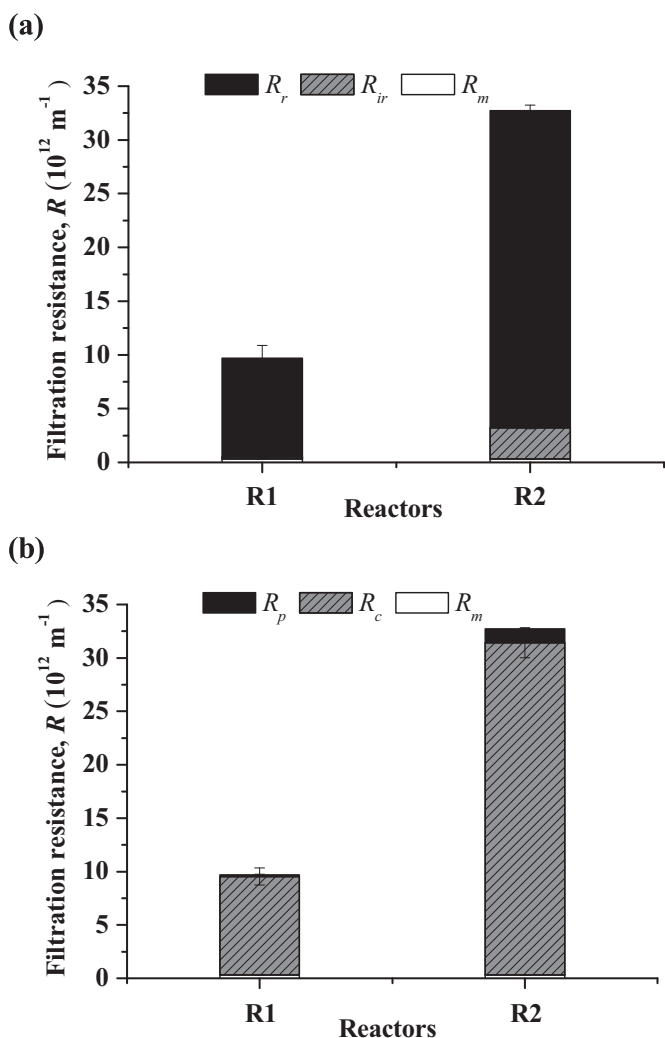
Fig. 4. Filtration resistance distributions on day 120: (a) Reversible, irreversible fouling resistance (R_r, R_{ir}) and membrane resistance (R_m); (b) Cake layer (R_c), pore blocking resistance (R_p), and membrane resistance (R_m).

at 2 L/(m² h) without aeration shear stress (R1), while the flux is not stabilizing and continues to decrease under shear conditions (R2). Although R2 experienced higher flux values and thus higher loads in the period of day 10–25 than R1, the differences between both reactors cannot be attributed to organic loads, since the flux value in R1 is stable at increasing time, and thus stable independent of the total organic load, which is not the case in R2.

3.3. Effect of aeration shear stress on the filtration resistance distribution

The membrane modules were taken out for resistance distribution analyses at the end of the operation (day 120). Fig. 4 (a) shows the total resistance (R_t), the hydraulically reversible (R_r) and hydraulically irreversible resistance (R_{ir}) at that point. The value of R_t in R2 (32.7×10^{12} m^{-1}) was 3.4 times higher than in R1 (9.7×10^{12} m^{-1}). The hydraulically reversible resistance (R_{ir}) accounted for a large proportion of R_t with a value of 9.2 and 29.5×10^{12} m^{-1} in R1 and R2, respectively. The hydraulically irreversible resistance (R_{ir}) was much higher in R2 (2.9×10^{12} m^{-1}) than in R1 (0.2×10^{12} m^{-1}). These results demonstrate that aeration shear stress increased the total filtration resistance compared with the control, which was related to an increase of hydraulically reversible and irreversible resistance. The analysis of cake layer

and pore blocking resistance, as determined by mechanical cleaning of the membrane surface, showed similar results: The total resistance was dominated by cake layer resistance, while both cake layer and pore blocking resistances were enhanced in the presence of shear (Fig. 4(b)). The values for R_c were 9.2×10^{12} m^{-1} and 31.1×10^{12} m^{-1} in R1 and R2, while R_p was 0.1×10^{12} m^{-1} and 1.3×10^{12} m^{-1} in R1 and R2, respectively.

3.4. Effect of aeration shear stress on the sludge properties

To explore the mechanisms of flux decline, the properties of the suspended sludge and the bio-fouling layer adhered on the membrane surface were investigated.

3.4.1. Morphology of the cake layer

Membrane modules from each reactor were taken out for OCT observation on day 35 and day 120. It can be seen from Fig. 5(a), (b), (e) and (f) and Table 1 that the thickness of the bio-fouling layer in both reactors increased with time. In R1 (with aeration shear) the average thickness increased from 275 ± 15 μm to 344 ± 70 μm, while in R2 it increased from 35 ± 1.8 μm to 129 ± 21 μm on day 35 and 120, respectively. Also the roughness of the cake layer increased with time, from 22.4 ± 5.6 μm to 121 ± 16 μm in R1, and from 3.2 ± 0.6 μm to 45.3 ± 9.1 μm in R2 on day 35 and 120, respectively. The roughness of the surface in R1 was significantly higher than that of R2 (3–7 fold). Thus, the aeration shear stress significantly reduces both the thickness and the roughness of the bio-fouling layer on the membrane. Furthermore, it can be seen from Fig. 5(a), (b), (e) and (f) that local detachment of the bio-fouling layer occurred in R1 (low shear) while the layer adhered tightly bound to the membrane surface in R2 (with aeration shear).

OCT was also used to analyze the fouling layer after hydraulic cleaning and chemical cleaning. It can be observed from Fig. 5(c), (d), (g) and (h) that most of the cake layer can be removed by gentle flushing of the membrane surface, whereby the thickness of the fouling layer was diminished from 344 ± 70 μm to 7.4 ± 1.4 μm in R1 (low shear) (Table 1). In R2 however, still a part of biofilm with an average thickness of 56.2 ± 2.3 μm remained bound to the membrane surface after hydraulic cleaning. For R1, no changes of the fouling layer structure could be observed after chemical cleaning, because the layer was already practically completely removed by hydraulic cleaning. In R2 (with aeration shear) however, chemical cleaning resulted in partial removal of the remaining fouling layer (decrease in thickness from 56.2 μm to 34.5 μm). Thus, it can be concluded that under shear conditions the bio-fouling layer adhered more strongly on the membrane surface than in absence of shear. These results correspond with the resistance analysis reported in Section 3.3 (higher reversible and irreversible resistance in presence of shear), which is probably related to the selection of organisms and/or an increase of EPS (see next section), resulting in a stronger adherence of the fouling layer to the membrane.

3.4.2. EPS analyses

It has been reported that SMP and EPS play a major role in membrane fouling in MBR systems [1,26], and therefore these parameters were also investigated in our study. At the end of the experiment, the concentrations of EPS in the suspended sludge and in the bio-fouling layer were measured by protein and polysaccharide measurements. As can be seen in Table 2, the suspended sludge EPS concentrations in the two reactors are quite similar and the differences are within the experimental error. However, there were significant differences between the EPS content in the bio-fouling cake of the two reactors. The EPS content in the cake of R2 was nearly two times as high as that in R1.
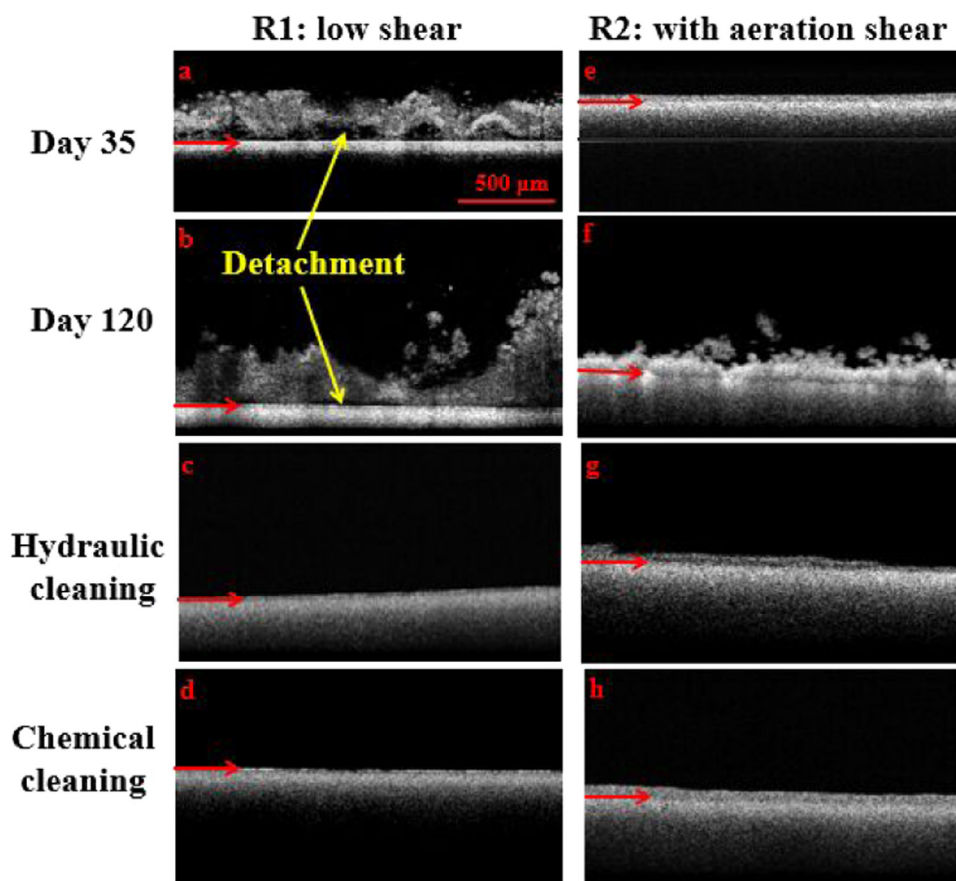
Fig. 5. Typical OCT images of the bio-fouling layer developed on the membrane surface on day 35 (a, e) and day 120 (b, f) after hydraulic cleaning (c, g) and after chemical cleaning (d, h) in R1 and R2. Red arrows indicate the interface between membrane and bio-fouling layer.

Table 1
Bio-fouling layer thickness and roughness as calculated from OCT image analyses in R1 (low shear) and R2 (with aeration shear) ($n=4$).

	Thickness (µm)		Roughness (µm)	
	R1	R2	R1	R2
Day 35	275 ± 15	35 ± 1.8	22.4 ± 5.6	3.2 ± 0.6
Day120	344 ± 70	129 ± 21	121 ± 16	45.3 ± 9.1
After Hydraulic cleaning	7.4 ± 1.4	56.2 ± 2.3	–	–
After Chemical cleaning	7.4 ± 1.4	34.5 ± 1.9	–	–

Table 2
EPS analyses in R1 (low shear) and R2 (with aeration shear) ($n=2$).

Days	Sludge	mgEPS/gVSS	mgPr/gVSS	mgPs/gVSS
120 d	R1 suspended sludge	106.3 ± 4.6	78.0 ± 3.5	12.7 ± 1.5
	R2 suspended sludge	92.1 ± 6.2	71.9 ± 1.0	13.4 ± 3.5
	R1 bio-fouling layer	122.9 ± 8.8	103.7 ± 0.7	24.7 ± 2.1
	R2 bio-fouling layer	234.8 ± 10.4	163.7 ± 3.6	30.9 ± 1.3

The protein contents were 103.7 and 163.7 mg bovine serum albumin (BSA) equivalents/g volatile suspended solids (VSS), respectively, while the polysaccharide contents were 24.7 and 30.9 mg glucose equivalents/g VSS, in R1 and R2 respectively. These results show that while the composition of suspended sludge is similar in both reactors, the membrane biofilm contains substantially more polysaccharides and proteins in the presence of shear than without aeration shear. This confirm the hypothesis put forward above, that shear stress results in a stronger adhesion of the bio-fouling layer which is accomplished by the production of more EPS.

In order to better understand whether the shear stress influenced the distribution of EPS in the cake layer, we conducted CLSM analyses. Z-stacks were rebuilt in three dimensions using *Imaris* software (Bitplane, Zurich, Switzerland) as shown in Fig. S2(a)–(j) in the Supplementary Material. Red, green and blue signals represent proteins, polysaccharides and bacterial cells (DNA), respectively. Fig. S2(a) and (b) are the images of bio-fouling layer of R1 and R2, respectively. It can be seen that the colour intensity and coverage of red, green and blue signals in Fig. S2(b) are stronger than in Fig. S2(a), which confirms the results presented before that the EPS content is higher under shear condition.

4. Discussion

4.1. Permeate flux stability

A membrane reactor based on the GDM principle (low pressure, no flushing, no biofilm removal) was tested for the treatment of synthetic grey water and compared with a similar system operated with aeration shear. The latter resembles a submerged MBR, apart from the fact that the TMP (50 mbar) was substantially lower than usually applied in MBRs. Our study shows that flux stabilization occurs during extended operation times in the reactor with low shear, but not in the system where the membranes are exposed to aeration shear. Furthermore, the data show that aeration shear stress resulted in a higher flux during the initial stage (40 days), while the flux was lower in the period afterwards and continued to decrease in case of aeration shear. In a recent study by Patsios et al. [27], it was concluded that under typical

hydrodynamic conditions in an MBR, flow shearing might be ineffective to cause biofouling layer detachment. Our results confirm this hypothesis, even showing that the operation with aeration shear stress leads to a lower permeability of the biofouling layer. In the reactor with low shear, the permeate flux stabilized at 2 L/(m² h). Similar results were reported by Jabornig and Podmirseg [28], showing that the flux stabilized without fouling control on a flux level of 1–2 L/(m² h) in a fixed hollow fibre biofilm membrane reactor. In former investigations with non-aerated GDM (Peter-Varbanets et al. [3]), it was reported that the flux stabilized in the range of 4–10 L/(m² h) for different types of surface water types and diluted wastewater (with a TOC of 2–15.3 mg/L). The stabilization of flux is related to biological activity within the fouling layer attached on the membrane surface, leading to the development of a heterogeneous bio-fouling layer [3,6,7]. Previous studies showed the stable flux value decreased with increasing TOC under non-aerated, but still aerobic conditions [4]. In our investigations, both reactors were aerated, which results in a TOC reduction of around 95%, from 100 mg/L in the feed to 5 mg/L in the effluent. The DOC concentration in the reactor was 10–15 mg/L (Fig. 1(b)). Thus, the conditions in the reactor with low shear (R1) are similar to those reported in earlier GDM investigations, although the stable flux values are slightly lower.

It should be noticed that the concept of stable flux in GDM is quite different from the concept of critical flux. The latter concept was first presented in a microfiltration system by Field [8] and Howell [29]. The critical flux was defined as the flux below which a decline of flux with time does not occur, while above it progressive fouling is observed. Le-Clech et al. [30] determined the critical flux using standard flux-step method in a submerged membrane bioreactor. In these studies the filtration time was limited to minutes or hours, while a flux decline (or trans-membrane pressure increase) took place over long-term (several days). In the concept of GDM, flux stabilization occurs on the time scale weeks or months [3], up to several years (non-published data). In contrast to critical flux, stable flux values in GDM are not related to physical phenomena only, but also to biological process in the biofouling layer (including predation) [6].

4.2. Relationship between fouling layer properties and permeate flux decline

In conventional cake filtration without biological activity, the hydraulic resistance of the cake layer increases with the thickness of the layer [31]. However, it can be seen from Fig. 5 and Table 2 that the thickness in R1 was higher than in R2, while the resistance was lower. We have identified two different factors which can explain these differences. First, as shown by OCT imaging, it can be observed that the morphology of the biofouling layer in R1 is characterized by a high heterogeneity and roughness, while even local detachment of the fouling layer occurred in this system (Day 120, Fig. 5(b)). This is confirmed by an investigation by Martin et al. [32], showing that a relationship between biofouling heterogeneity and flux exists. Biofilm analysis was also conducted by Jabornig and Podmirseg [28], which revealed numerous nematodes, sheathed bacteria and protozoa which form spongy, woven-like and porous biofilm structures under no aeration shear conditions. Secondly, as shown in Table 2, the bio-fouling layer in the system with shear showed a higher content of EPS than in the system with low shear. EPS and SMP consist of polysaccharides, proteins, lipids and nucleic acids, which originate from cell lysis, microbial metabolites or unmetabolized wastewater components [33]. Usually, proteins and polysaccharides are assumed to be the major components that contribute to membrane fouling [34]. While differences were observed in the bio-fouling layer, no

significant differences could be observed between the EPS and SMP concentrations in the bulk sludge of both reactors (Table 2). Similar results were reported by Lee et al. [35], who concluded that the EPS directly affected the decrease in the permeate flux, which resulted in membrane clogging and causing high filtration resistance.

With regard to the filtration resistance distribution, we found that the main part of the fouling resistance is within the bio-fouling layer, which can be removed hydraulically (Fig. 4). It was reported before that during long-term GDM operation, excessively accumulated bio-fouling layer was sloughing off even by gravity, which led to a temporal flux recovery [4]. Furthermore, we observed that both reversible fouling and irreversible fouling are considerably higher with aeration shear (R2) than at low shear conditions (R1), which can probably be explained by the fact that bacteria are selected which adhere strongly to the membrane and excrete much EPS, which leads to irreversible fouling. This hypothesis can be supported by several studies [14,36], showing that EPS not only contributes to reversible fouling, but also causes irreversible fouling phenomena in MBR processes.

In summary, the aeration shear stress leads to an increased reversible and irreversible resistance of the bio-fouling layer, which can be explained by the higher content of EPS and differences in biofilm morphology.

4.3. Comparison with other studies

As mentioned in Section 1, SADm is an important parameter to evaluate the aeration conditions. Air injection reduced fouling in an SMBR up to a critical flow rate corresponding to a SADm of 250 L/h m². Beyond this value, increasing airflow did not have a positive effect on TMP, which was linked with the cake removal efficiency [9]. It has been shown by Meng et al. [11] that excessive aeration (800 L/h, SADm of 8000 L/h m²) resulted in floc breakage and promoted the release of colloids and solutes in SMBRs filtrating synthetic wastewater, resulting in stronger membrane fouling. In this study, the SADm was set at 1000 L/h m² (higher than the critical SADm), and could remove the fouling layer efficiently.

Previous studies show that appropriate increase of aeration intensity would lead to a higher flux or lower fouling rate [10,13], which is in contradiction to our results. The reason for this is that in previous studies an increased aeration intensity also led to an increased DO concentration, which retarded the membrane fouling rate [17]. However, we separated the aeration diffuser from the membrane surface in the control reactor (R1), to avoid the influence of DO on the properties of suspended sludge and fouling layer. Secondly, our reactors were operated without any backwash and physical cleaning, while normal MBRs are operated with cycles consisting of several minutes of drawing and several minutes of back washing. The back wash would provide an additional counterforce on the fouling layer, which would lead to a different mechanism for the fouling layer formation. Thirdly, the operation pressure of our system (constant pressure of 50 mbar) was much lower than that in normal MBRs operated with constant flux (100–600 mbar) [37–39]. Due to these different aeration regimes and operation conditions, the aeration shear in our system caused more severe fouling and resulted in a continuously decreasing flux, while the low-shear reactor remained at a constant flux during long-term operation (day 40–120).

4.4. Mechanisms of aeration shear stress exacerbating membrane fouling

To better understand the underlying mechanism of shear stress accelerating the membrane fouling, we discuss the formation of

the fouling layer from both the physical and the biological perspectives.

4.4.1. Influence of physical processes

As shown in Section 3.4.1, the average thickness of the fouling layer under aeration shear stress conditions was smaller than that at low shear stress. It can be assumed that the shear caused by the air bubbles continuously removed the part of the bio-fouling layer from the membrane surface which was loosely bound, while the tightly bound material adhered on the membrane surface. This results in a continuous accumulation of tightly bound material on the membrane, and the formation of a compact, "sticky" bio-fouling layer during long term operation. In the absence of shear stress, the accumulation of material on the membrane surface is a result of deposition only and no selection of strongly attaching material and bacteria takes place.

4.4.2. Influence of biological processes

From the results of EPS analyses, it can be seen that the aeration shear stress increased the contents of EPS, polysaccharides and proteins in the bio-fouling layer, as compared to the reactor with low shear (Table 2). We can postulate that the shear conditions led to selection of strongly binding micro-organisms, while the higher EPS content is related to this binding capacity and the high resistance of the fouling layer. Ying et al. [40] and Al Ashhab et al. [41] studied the bio-fouling of reverse-osmosis (RO) membranes during the treatment of tertiary wastewater at different shear rates generated by different velocities of the feed water. Similar to our results, they found that at high shear rates, the bacterial community of the biofilm consisted mainly of populations known to excrete high amounts of EPS. In summary, the aeration shear stress resulted in an increase of the EPS contents (proteins and polysaccharides) in the bio-fouling layer. The higher total EPS content can be related to the fact that aeration shear stress decreased the permeate flux and accelerated the membrane fouling.

It is expected that the findings presented here can be useful not only for GDMBR development but also for the development of strategies to reduce fouling and increase fluxes in conventional MBRs during wastewater treatment. In order to control the membrane fouling, it is suggested to locate the aeration diffuser spatially separated from the membrane modules. It should be evaluated if this is leading to reduced fouling only in low pressure membrane systems operated without back flushing or in MBRs in general. Furthermore, it would be useful to analyze the composition of the microbial community under different shear conditions in order to better understand the fouling mechanisms.

5. Conclusions

A low pressure, gravity driven membrane reactor was evaluated for the treatment of synthetic grey water. One reactor was operated with and one reactor was operated without aeration shear stress at the membrane surface. High shear condition resulted in a thinner but denser bio-fouling layer with a higher EPS content (proteins and polysaccharides), more reversible and irreversible fouling and a lower flux than in the absence of aeration shear stress. In the latter case, the flux stabilized at a value of around 2.0 L/(m^2 h) after 40 days of operation, and remained constant until the end of the experiment without using any cleaning or back flushing, while the flux continued to decrease in the case of high shear, reaching a value of 0.5 L/(m^2 h) at the end of the experiment (120 days). Thus, the reactor with low shear stress can be operated with low maintenance (without any backwash, physical flushing or chemical cleaning) during extended periods of time, which makes this suitable for decentralized wastewater treatment and reuse, although the flux is significantly lower compared to MBRs. The results presented here can have important implications for improving the flux and decreasing the energy consumption of wastewater treatment.

Appendix A. Supplementary material

Supplementary data associated with this article can be found in the online version at http://dx.doi.org/10.1016/j.memsci.2016.03.025.

References

[1] F. Meng, S.R. Chae, A. Drews, M. Kraume, H.S. Shin, F. Yang, Recent advances in membrane bioreactors (MBRs): membrane fouling and membrane material, Water Res. 43 (2009) 1489–1512.
[2] E. Braak, M. Alliet, S. Schetrite, C. Albasi, Aeration and hydrodynamics in submerged membrane bioreactors, J. Membr. Sci. 379 (2011) 1–18.
[3] M. Peter-Varbanets, F. Hammes, M. Vital, W. Pronk, Stabilization of flux during dead-end ultra-low pressure ultrafiltration, Water Res. 44 (2010) 3607–3616.
[4] M. Peter-Varbanets, J. Margot, J. Traber, W. Pronk, Mechanisms of membrane fouling during ultra-low pressure ultrafiltration, J. Membr. Sci. 377 (2011) 42–53.
[5] M. Boulestreau, E. Hoa, M. Peter-Verbanets, W. Pronk, R. Rajagopaul, B. Lesjean, Operation of gravity-driven ultrafiltration prototype for decentralised water supply, Desalin. Water Treat. 42 (2012) 125–130.
[6] N. Derlon, M. Peter-Varbanets, A. Scheidegger, W. Pronk, E. Morgenroth, Predation influences the structure of biofilm developed on ultrafiltration membranes, Water Res. 46 (2012) 3323–3333.
[7] N. Derlon, N. Koch, B. Eugster, T. Posch, J. Pernthaler, W. Pronk, E. Morgenroth, Activity of metazoa governs biofilm structure formation and enhances permeate flux during Gravity-Driven Membrane (GDM) filtration, Water Res. 47 (2013) 2085–2095.
[8] R.W. Field, D. Wu, J.A. Howell, B.B. Gupta, Critical flux concept for microfiltration fouling, J. Membr. Sci. 100 (1995) 259–272.
[9] T. Ueda, K. Hata, Y. Kikuoka, O. Seino, Effects of aeration on suction pressure in a submerged membrane bioreactor, Water Res. 31 (1997) 489–494.
[10] F. Fan, H. Zhou, Interrelated effects of aeration and mixed liquor fractions on membrane fouling for submerged membrane bioreactor processes in wastewater treatment, Environ. Sci. Technol. 41 (2007) 2523–2528.
[11] F. Meng, F. Yang, B. Shi, H. Zhang, A comprehensive study on membrane fouling in submerged membrane bioreactors operated under different aeration intensities, Sep. Purif. Technol. 59 (2008) 91–100.
[12] J.P. Nywening, H. Zhou, Influence of filtration conditions on membrane fouling and scouring aeration effectiveness in submerged membrane bioreactors to treat municipal wastewater, Water Res. 43 (2009) 3548–3558.
[13] R.S. Trussell, R.P. Merlo, S.W. Hermanowicz, D. Jenkins, Influence of mixed liquor properties and aeration intensity on membrane fouling in a submerged membrane bioreactor at high mixed liquor suspended solids concentrations, Water Res. 41 (2007) 947–958.
[14] H.Y. Kim, K.M. Yeon, C.H. Lee, S. Lee, T. Swaminathan, Biofilm structure and extracellular polymeric substances in low and high dissolved oxygen membrane bioreactors, Sep. Sci. Technol. 41 (2006) 1213–1230.
[15] B.M. Wilén, P. Balmér, The effect of dissolved oxygen concentration on the structure, size and size distribution of activated sludge flocs, Water Res. 33 (1999) 391–400.
[16] M.A. Yun, K.M. Yeon, J.S. Park, C.H. Lee, J. Chun, D.J. Lim, Characterization of biofilm structure and its effect on membrane permeability in MBR for dye wastewater treatment, Water Res. 40 (2006) 45–52.
[17] Y.L. Jin, W.N. Lee, C.H. Lee, I.S. Chang, X. Huang, T. Swaminathan, Effect of DO concentration on biofilm structure and membrane filterability in submerged membrane bioreactor, Water Res. 40 (2006) 2829–2836.
[18] A. Campesi, M.O. Cerri, C.O. Hokka, A.C. Badino, Determination of the average shear rate in a stirred and aerated tank bioreactor, Bioprocess Biosyst. Eng. 32 (2009) 241–248.
[19] C. Diaper, M. Toifl, M. Storey, Greywater technology testing protocol, CSIRO:

Water for a Healthy Country, National Research Flagship Report Series, 2008.

[20] L.D. Nghiem, N. Oschmann, A.I. Schäfer, Fouling in greywater recycling by direct ultrafiltration, Desalination 187 (2006) 283–290.

[21] S.S. Adav, D.J. Lee, Extraction of extracellular polymeric substances from aerobic granule with compact interior structure, J. Hazard. Mater. 154 (2008) 1120–1126.

[22] P.K. Smith, R.I. Krohn, G.T. Hermanson, A.K. Mallia, F.H. Gartner, M. D. Provenzano, E.K. Fujimoto, N.M. Goeke, B.J. Olson, D.C. Klenk, Measurement of protein using bicinchoninic acid, Anal. Biochem. 150 (1985) 76–85.

[23] M. DuBois, K.A. Gilles, J.K. Hamilton, P.A. Rebers, F. Smith, Colorimetric method for determination of sugars and related substances, Anal. Chem. 28 (1956) 350–356.

[24] K. Listiarini, W. Chun, D.D. Sun, J.O. Leckie, Fouling mechanism and resistance analyses of systems containing sodium alginate, calcium, alum and their combination in dead-end fouling of nanofiltration membranes, J. Membr. Sci. 344 (2009) 244–251.

[25] X.-y Li, X.-m Wang, Modelling of membrane fouling in a submerged membrane bioreactor, J. Membr. Sci. 278 (2006) 151–161.

[26] A. Drews, Membrane fouling in membrane bioreactors—characterisation, contradictions, cause and cures, J. Membr. Sci. 363 (2010) 1–28.

[27] S.I. Patsios, T.B. Goudoulas, E.G. Kastrinakis, S.G. Nychas, A.J. Karabelas, A novel method for rheological characterization of biofouling layers developing in Membrane Bioreactors (MBR), J. Membr. Sci. 482 (2015) 13–24.

[28] S. Jabornig, S.M. Podmirseg, A novel fixed fibre biofilm membrane process for on-site greywater reclamation requiring no fouling control, Biotechnol. Bioeng. 112 (2015) 484–493.

[29] J.A. Howell, Sub-critical flux operation of microfiltration, J. Membr. Sci. 107 (1995) 165–171.

[30] P. Le Clech, B. Jefferson, I.S. Chang, S.J. Judd, Critical flux determination by the flux-step method in a submerged membrane bioreactor, J. Membr. Sci. 227 (2003) 81–93.

[31] Y. Gao, S. Haavisto, W. Li, T. Chuyang, J. Salmela, A.G. Fane, A. Novel, Approach to characterizing the growth of a fouling layer during membrane filtration via optical coherence tomography, Environ. Sci. Technol. (2014).

[32] K.J. Martin, D. Bolster, N. Derlon, E. Morgenroth, R. Nerenberg, Effect of fouling layer spatial distribution on permeate flux: a theoretical and experimental study, J. Membr. Sci. 471 (2014) 130–137.

[33] H.C. Flemming, J. Wingender, Relevance of microbial extracellular polymeric substances (EPSs)-Part I: structural and ecological aspects, Water Sci. Technol. (2001) 1–8.

[34] C. Dreszer, J.S. Vrouwenvelder, A.H. Paulitsch-Fuchs, A. Zwijnenburg, J. C. Kruithof, H.C. Flemming, Hydraulic resistance of biofilms, J. Membr. Sci. 429 (2013) 436–447.

[35] D.-Y. Lee, Y.-Y. Li, T. Noike, G.-C. Cha, Behavior of extracellular polymers and bio-fouling during hydrogen fermentation with a membrane bioreactor, J. Membr. Sci. 322 (2008) 13–18.

[36] C. Huyskens, E. Brauns, E. Vanhoof, H. Dewever, A new method for the evaluation of the reversible and irreversible fouling propensity of MBR mixed liquor, J. Membr. Sci. 323 (2008) 185–192.

[37] Z. Wang, J. Ma, C.Y. Tang, K. Kimura, Q. Wang, X. Han, Membrane cleaning in membrane bioreactors: a review, J. Membr. Sci. 468 (2014) 276–307.

[38] C.-H. Wei, X. Huang, R. Ben Aim, K. Yamamoto, G. Amy, Critical flux and chemical cleaning-in-place during the long-term operation of a pilot-scale submerged membrane bioreactor for municipal wastewater treatment, Water Res. 45 (2011) 863–871.

[39] P. Le-Clech, V. Chen, A.G. Fane, Fouling in membrane bioreactors used in wastewater treatment, J. Membr. Sci. 284 (2006) 17–53.

[40] W. Ying, V. Gitis, J. Lee, M. Herzberg, Effects of shear rate on biofouling of reverse osmosis membrane during tertiary wastewater desalination, J. Membr. Sci. 427 (2013) 390–398.

[41] A. Al Ashhab, O. Gillor, M. Herzberg, Biofouling of reverse-osmosis membranes under different shear rates during tertiary wastewater desalination: Microbial community composition, Water Res. 67 (2014) 86–95.